



Contents lists available at ScienceDirect

Journal of Organometallic Chemistry

journal homepage: www.elsevier.com/locate/jorganchem

Cobalt-promoted B–H and C–H activation in the three-component reactions of 16-electron cobalt carboranedithiolate, alkyne and bronsted acids

Rui Zhang, Lin Zhu, Zhenzhong Lu, Hong Yan*

State Key Laboratory of Coordination Chemistry, School of Chemistry and Chemical Engineering, Nanjing University, Nanjing 210093, Jiangsu, China

ARTICLE INFO

Article history:

Received 28 March 2015

Received in revised form

6 June 2015

Accepted 8 June 2015

Available online xxx

Dedicated to Prof. Russell Grimes on the occasion of his 80th birthday.

Keywords:

B–H activation

Cobalt

Carborane

Alkyne

Bronsted acid

ABSTRACT

The three-component reactions of $\text{Cp}^\# \text{Co}(\text{S}_2\text{C}_2\text{B}_{10}\text{H}_{10})$ ($\text{Cp}^\# = \text{Cp}$, **1a**; MeCp , **1b**; Me_4Cp , **1c**; Me_5Cp , **1d**), methyl propiolate (**2**) and Bronsted acid organic ligands (**L1–L8**) are reported. Only can **1a** and **1b** lead to selective B-functionalization at carborane with cyclopentadienyl or methyl-cyclopentadienyl as a functional group at ambient temperature in good yields. Four types of products containing a coupled B–C bond are obtained dependent on the type of the used Bronsted acids (**L1–L8**). If stronger coordinating ligands **L1–L3** are chosen compounds **3a(L1–L3)** and **3b(L1–L3)** are isolated where **L1–L3** loses one proton to provide 3 electrons to metal and alkyne is reduced to olefin. If **L4** and **L5** are used, products **4a** or **4b** are generated where the Bronsted acid is not observed but the alkyne is reduced to sp^3 and forms a five-membered ring with Co center. Allenes (**L6** and **L7**) lead to **5a(L6)** and **5a(L7)** where an allyl unit is coordinated to metal. In case of CpH (**L8**), compounds **6a** and **6b** are produced which contains an *in-situ* generated unusual carborane-functionalized dithiolate ligand from 4 + 2 cycloaddition of alkyne and the added cyclopentadiene. All products were fully characterized by spectroscopic techniques and elemental analysis. All products were fully characterized and some typical solid-state structures were further determined by X-ray crystallographic analysis. The co-promoted mechanisms by metal and Bronsted acids to lead both B–H and C–H activation are proposed on the basis of deuterium labeling as well as NMR, MS, GC monitoring experiments.

© 2015 Published by Elsevier B.V.

1. Introduction

Derivatives of polyhedral boranes have been widely applied in the areas of materials, medicine, catalysis, etc. [1–15] and arouse great interests among the researches on their functionalization. However, selective and straightforward boron substitutions have been proven difficult [16,17], although significant advances in metal-promoted or metal-catalyzed hydroboration of polyhedral boranes have been achieved [18–37]. $\text{Cp}^\# \text{M}(\text{E}_2\text{C}_2\text{B}_{10}\text{H}_{10})$ ($\text{M} = \text{Co}$, Rh , Ir ; $\text{E} = \text{S}$, Se) reacted with active alkynes to achieve the selective hydroboration of *o*-carborane have been well known [26–32]. The metal center, chalcogen element and reagents are all important to decide the reactivity of these 16e half-sandwich compounds. It has been found that cobalt species are much more reactive than their analogous rhodium and iridium species [33,34,37,38]; the

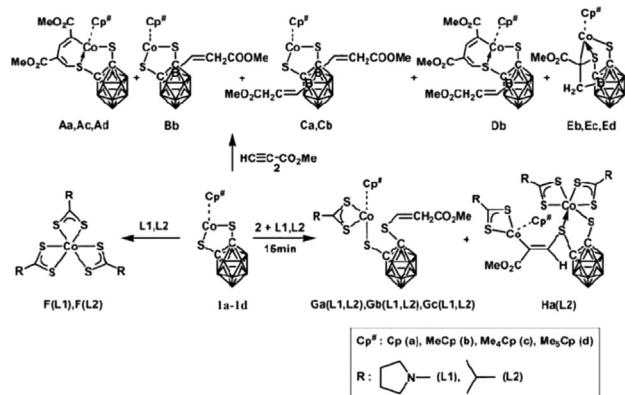
dithiolate compounds are more reactive than diselenolate species; electron-deficient alkynes are more reactive than electron-rich alkynes [39,40].

In the case of $\text{Cp}^\# \text{Co}(\text{S}_2\text{C}_2\text{B}_{10}\text{H}_{10})$ ($\text{Cp}^\# = \text{Cp}$, MeCp , Me_4Cp , Me_5Cp) [41], different size of the ancillary ligand could lead to different type of products (Scheme 1). Compounds with smaller size ligands Cp and MeCp prefer the B-substituted products at carborane, whereas the larger ligands Me_4Cp , Me_5Cp give rise to the products of alkyne two-fold insertion into a M–S bond. In three-component reactions if a third chelating dithio-ligand is added, the reactivity decreases with the size increase of ancillary ligand. The type of generated products is dependent on the competition between alkyne and dithio-ligand, and determined by steric and electronic effects of these reagents.

Through control of reaction ratio of the three-component reactions of $\text{Cp}^\# \text{Co}(\text{S}_2\text{C}_2\text{B}_{10}\text{H}_{10})$ ($\text{Cp}^\# = \text{Cp}$, MeCp , Me_4Cp , Me_5Cp), methyl propiolate and dithio ligands the three-component products **G**, **H** and two-component compounds **F** were obtained (Scheme 1) [41]. Also, we have isolated novel compounds with B–C

* Corresponding author.

E-mail address: hyan1965@nju.edu.cn (H. Yan).



Scheme 1. Two-component reaction between **1a–1d** and **2** (up); two component-reaction between **1a–1d** and **L1/L2** (left); and three-component reaction of **1a–1d**, **2** and **L1/L2** (right) [41].

coupling which are generated via both C–H and B–H activation [42]. Herein, the range of reactions and details are reported.

2. Results and discussions

2.1. Synthesis and structure

The Bronsted acid organic ligands (**L1–L8**) were introduced to two component reactions of 16e complexes $\text{Cp}^{\#}\text{Co}(\text{S}_2\text{C}_2\text{B}_{10}\text{H}_{10})$ ($\text{Cp}^{\#} = \text{Cp}$, **1a**; MeCp, **1b**; Me₄Cp, **1c**; Me₅Cp, **1d**) and methyl propiolate (**2**), as a result, a series of novel products containing B–C coupling between carborane cage and $\text{Cp}^{\#}$ (**1a** and **1b**) unit were generated at ambient temperature (Scheme 2).

Small organic ligands play vital roles in the formation of adducts with a coupled B–C bond. The 4e donor chelating ligands such as

2,2-bipyridine and 1,10-phenanthroline did not lead to similar products, reflecting the requirement of electron accounting of the metal center. Owing to the different strength of these potential 3e donor ligands (**L1–L8**) in coordination to Co metal center, four types of products were defined (Scheme 2). All the products were fully characterized by spectroscopic data and the solid-state structures of some typical compounds were determined by using X-ray crystallography. No B–C coupling products could be isolated in the cases of **1c** and **1d** starting compounds because of the steric problem of the ancillary ligands.

2.1.1. 3a(L1–L3) and 3b(L1–L3)

As shown in Scheme 2 and Fig. 1 **3a(L1)** is the first example of

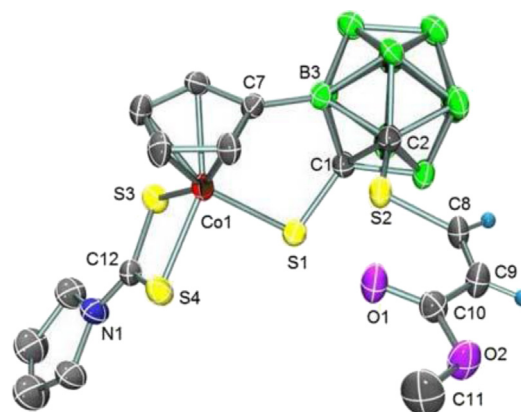
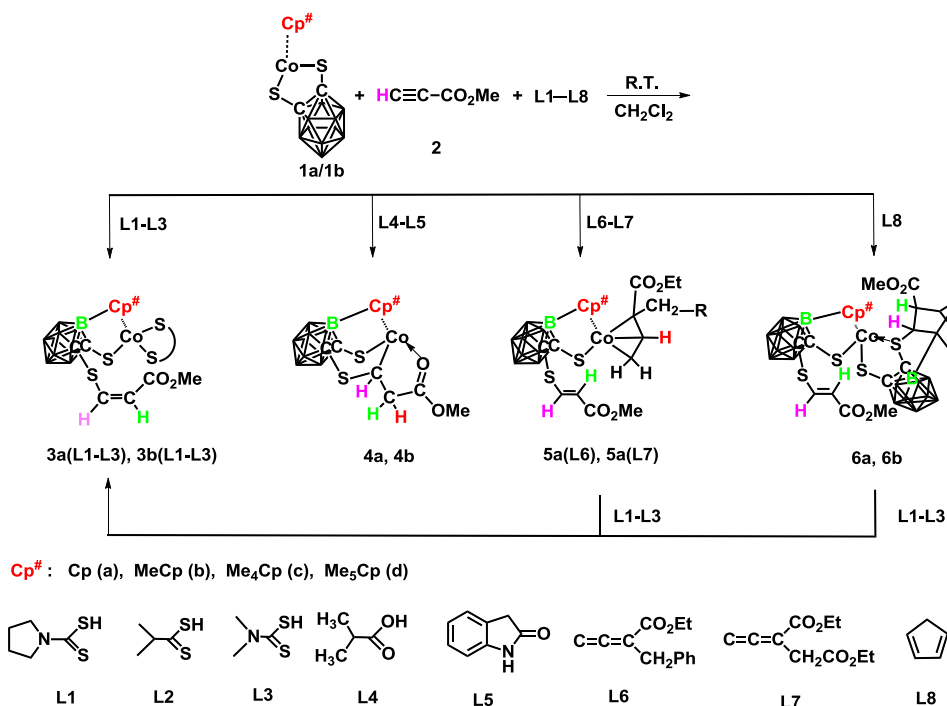


Fig. 1. Molecular structure of **3a(L1)**; ellipsoids show 30% probability levels, and some of the hydrogen atoms have been omitted for clarity. Selected bond lengths (Å) and angles (°): Co1–ring centroid 1.682(1), C1–C2 1.843(6), B3–C7 1.569(6), C1–S1 1.740(4), C2–S2 1.778(4), C8–C9 1.333(5), C8–S2 1.730(4), C12–S3 1.696(4), C12–S4 1.708(4), C12–N1 1.314(5), Co1–S4 2.246(1), Co1–S3 2.258(1), Co1–S1 2.272(1), B3–C2 1.724(6), C3–B3–C2 124.8(4), B3–C2–S2 114.2(3), C9–C8–S1 124.1(3), C8–C9–C10 123.8(4), S3–C12–S4 111.1(3), C3–Co1–S2 89.4(1), S4–Co1–S3 77.1(1).



Scheme 2. Reactions of **1a/1b**, **2** and **L1–L8** at ambient temperature lead to four types of products.

this type of products. The carborane cage is linked to the Cp ring through a covalent B–C bond with a length of 1.569(6) Å. The substituted Cp ring remains coordinated to Co metal center in an η^5 -mode. Pyrrolidine-1-carbodithioic acid (**L1**) has lost one hydrogen atom and chelated to Co as a 3e donor. The alkyne has been reduced to an olefinic unit in a *Z* configuration and is connected to one S atom rather than a B atom as in compounds **B** and **C** (Scheme 1) [41] (Scheme 2). Clearly, the breakage of the rigid S-chelating binding in **1a** is essential for constructing the intramolecular coupling of the carborane-dithiolate and cyclopentadienyl moieties.

Spectroscopic analysis of **3a(L1)** confirms that the relevant features of its solid-state structure are retained in solution. In contrast to one singlet at 5.26 ppm for Cp group in **1a** [43] in the ^1H NMR spectrum, four well-separated signals at 6.01, 5.92, 5.24 and 4.97 ppm were assigned to the substituted Cp group in **3a(L1)**. The ^{13}C resonances of the substituted Cp ring appear at 91.0, 84.7, 84.3 and 83.8 ppm for those four C–H bonds, which was only one signal in **1a** [43] at 81.8 ppm. Moreover the characteristic broad ^{13}C resonance of the B–C bond is remarkably low-field shifted to 127.0 ppm, corresponding to the electron-deficient nature of B atom. The ^{11}B signal of the B–C bond (2.1 ppm) is also low-field shifted by 7–11 ppm in comparison to those in **1a** [43] further supporting the formation of a B–C bond. The reactions of **1a**, **2**, **L2** (or **L3**) led to **3a(L2)** and **3a(L3)** which have the similar spectroscopic data as for **3a(L1)** (see Supporting information II). The single-crystal X-ray diffraction of **3a(L2)** presents in Fig. 2, revealing the similar Cp–carborane cage coupling moiety.

Compounds **3b(L1–L3)** have the similar structures as **3a(L1–L3)**. The only difference is that Cp ring is replaced by MeCp. But interestingly, the C–H bond of the *ortho*-position of the methyl unit is activated as shown in **3b(L3)** (Fig. 3) with the B–C bond length of 1.586(7) Å. The NMR data support the solid-state structure. In the ^1H NMR spectrum only three peaks show at 6.10, 5.55, 4.31 ppm corresponding to the three C–H units of MeCp ring. The ^{13}C NMR data display a broad resonance at 126.2 ppm for C–B bond, a sharp resonance at 108.6 ppm for another quaternary carbon and three sharp resonances at 96.6, 83.5 and 77.6 ppm for C–H units, as confirmed by 2D $^{13}\text{C}/^1\text{H}$ HETCOR (HMQC) experiments.

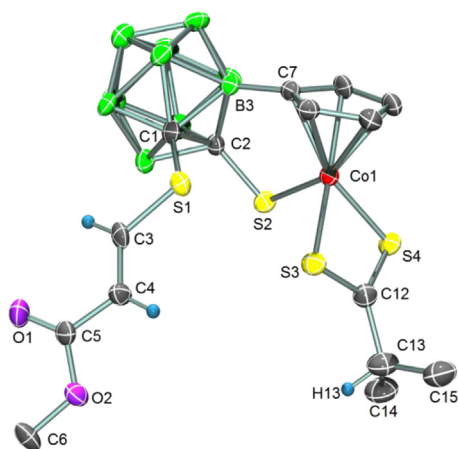


Fig. 2. Molecular structure of **3a(L2)**; ellipsoids show 30% probability levels, and some of the hydrogen atoms have been omitted for clarity. Selected bond lengths (Å) and angles ($^\circ$): Co1–ring centroid 1.685(1), C1–C2 1.793(8), B3–C7 1.564(1), C1–S2 1.780(8), C2–S1 1.761(8), C3–C4 1.321(1), C3–S1 1.752(7), C4–C5 1.486(1), C12–C13 1.523(1), C12–S4 1.659(8), C12–S3 1.677(8), Co1–S3 2.244(2), Co1–S4 2.254(2), Co1–S2 2.270(2), C7–B3–C2 112.8(6), S1–C1–C2 116.9(5), S2–C2–C1 118.4(5), C4–C3–S1 121.6(7), C3–C4–C5 117.0(8), S4–C12–S3 110.9(5), S3–Co1–S4 75.29(8), C3–S1–C1 102.7(4), C2–S2–Co1 104.2(3), C12–S3–Co1 86.9(3), C12–S4–Co1 87.0(3).

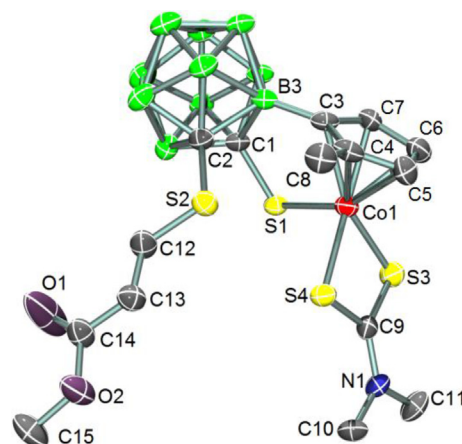


Fig. 3. Molecular structure of **3b(L3)**; ellipsoids show 30% probability levels, and the hydrogen atoms have been omitted for clarity. Selected bond lengths (Å) and angles ($^\circ$): Co1–ring centroid 1.696(1), B3–C3 1.586(7), C1–S1 1.764(6), C1–C2 1.788(6), C2–S2 1.769(4), C4–C8 1.476(7), C9–N1 1.313(6), C9–S3 1.710(5), C9–S4 1.722(5), C10–N1 1.462(6), C11–N1 1.453(6), C12–C13 1.267(7), C12–S2 1.720(5), C13–C14 1.453(7), C14–O1 1.260(12), C14–O2 1.294(6), Co1–S3 2.256(1), Co1–S4 2.274(1), Co1–S1 2.297(1), C3–B3–C1 112.2(4), S3–C9–S4 109.8(3), C13–C12–S2 125.0(4), C12–C13–C14 125.1(5), C11–N1–C10 116.9(4), C1–S1–Co1 104.4(1), C12–S2–C2 104.4(2).

2.1.2. 4a and 4b

The reactions of **1a/1b**, methyl propiolate (**2**) and **L4/L5** gave rise to the new compounds **4a/4b** (Scheme 2). The weakly coordinating **L4** and **L5** also lead to products with the B–C bond formation (**4a** and **4b**), but the ligand does not appear in the structure. Here, **L4** and **L5** might be considered as Bronsted acid catalysts. The solid-state structure of **4a** is given in Fig. 4. Instead of the strong ligand chelating to Co in **3a(L1–L3)/3b(L1–L3)**, the newly generated unit donates 3e to metal and form the five-membered ring Co1–C3–C4–C5–O1. The alkyne is reduced to alkane with 1.526 Å bond length of C3–C4. The NMR data are consistent with the solid structure of **4a**. The substituted Cp ring shows four signals at 6.40, 6.10, 5.49, 5.15 ppm in ^1H NMR and at 104.9, 100.8, 96.1, 78.6 ppm in ^{13}C NMR. The resonance of B–C bond presents remarkably low-field shifted as a characteristic broad signal at 127.2 ppm in ^{13}C NMR. The ^{11}B signal of the B–C bond appears at 4.5 ppm in ^{11}B NMR. The reduced alkyne coordinating to metal forms a five-membered ring which makes the structure more rigid. The

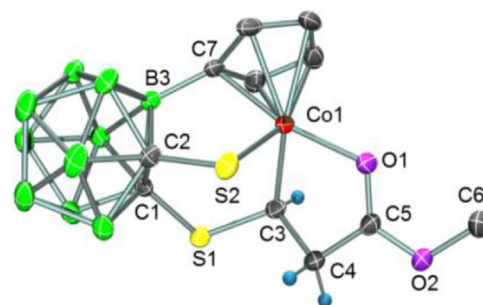


Fig. 4. Molecular structure of **4a**; ellipsoids show 30% probability levels, and some of the hydrogen atoms have been omitted for clarity. Selected bond lengths (Å) and angles ($^\circ$): Co1–ring centroid 1.686(1), B3–C7 1.549(3), C1–C2 1.680(3), C1–S1 1.768(2), C2–S2 1.786(2), C3–C4 1.526(3), C3–S1 1.799(2), C3–Co1 1.962(2), C4–C5 1.496(4), C5–O1 1.233(3), C5–O2 1.299(3), C6–O2 1.445(3), Co1–O1 1.983(8), Co1–S2 2.286(1), C7–B3–C2 119.3(1), C7–B3–C1 112.9(2), C1–C2–S2 117.3(1), C4–C3–S1 112.4(1), C4–C3–Co1 106.4(1), S1–C3–Co1 118.1(1), C5–C4–C3 106.3(2), O1–C5–O2 122.4(2), O1–C5–C4 120.4(2), C3–Co1–O1 84.1(1), O1–Co1–S2 94.1(1), C5–O1–Co1 112.5(1), C1–S1–C3 109.7(1), C2–S2–Co1 97.7(1).

proton at C(3) is coupled by the two adjacent non-equivalent hydrogen atoms, displaying *dd* coupling pattern at 6.85 ppm with $J_1 = 6.2$ Hz and $J_2 = 9.6$ Hz. The chemical shifts of the two hydrogen atoms at C(4) show at 3.17 ppm (*dd*, $J_1 = 9.6$ Hz, $J_2 = 18.5$ Hz) and 2.70 ppm (*dd*, $J_1 = 6.2$, $J_2 = 18.5$ Hz), respectively, which were further confirmed by 2D COSY and HMQC (SI-Figure 1). Compound **4b** is fully characterized by spectroscopic data (see Supporting information II).

2.1.3. 5a(L6) and 5a(L7)

The reactions of **1a**, **2** and **L6/L7** led to **5a(L6)/5a(L7)**. The solid-state structure of **5a(L6)** (Fig. 5) shows similar structural type to **3a(L1–L3)** except that the coordinating ligand is the 3e donor of allyl unit instead of dithio ligand in **3a(L1–L3)**. The ^1H signal of C9–H in **5a(L6)** shows *dd* coupling pattern at 6.10 ppm with $J_1 = 8$ Hz and $J_2 = 14$ Hz. The chemical shifts of the two hydrogen atoms at C8 atom appear at 5.20 ppm ($J = 8$ Hz) and 1.74 ppm ($J = 14$ Hz), respectively, further confirming the existence of the allyl group generated from ligand **L6**. The characteristic broad resonance at 126.8 ppm is attributed to the C–B bond in the ^{13}C NMR and the ^{11}B signal at 2.2 ppm corresponds to the B–C bond in ^{11}B NMR, indicating that the Cp has been connected to carborane at boron site. Compound **5a(L7)** is also fully characterized by spectroscopic data, similar to **5a(L6)** (see Supporting information).

2.1.4. 6a and 6b

The reactions of **1a/1b**, **2** and **L8** at ambient temperature led to **6a/6b** (Scheme 2). Cyclopentadiene (**L8**) is a very weak Bronsted acid, to our surprise, it can also produce the B–C coupled complexes. Two carborane cages shows in the solid structure of **6a** in each molecule (see Fig. 6). An unusual in situ-generated 3e donor *o*-carborane dithio ligand appears which bears a moiety formed by a [4 + 2] Diels–Alder cycloaddition, similar to the dithio ligands in **3a(L1–L3)/3b(L1–L3)**. Cp ring remains the η^5 -mode binding to metal and the lengths of the newly-generated characteristic B–C bonds are 1.576 Å for B(13)–C(5) and 1.559 Å for B(3)–C(14), respectively.

The NMR data are in agreement with the solid-state structure.

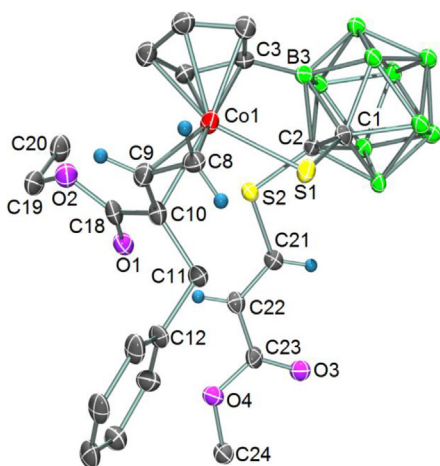


Fig. 5. Molecular structure of **5a(L6)**; ellipsoids show 30% probability levels, and some of the hydrogen atoms have been omitted for clarity. Selected bond lengths (Å) and angles (°): Co1–ring centroid 1.684(1), B3–C3 1.596(4), C1–S1 1.753(3), C1–C2 1.802(4), C2–S2 1.750(3), C8–C9 1.434(4), C8–Co1 2.105(3), C9–C10 1.411(4), C9–Co1 2.017(3), C10–C18 1.469(4), C10–C11 1.554(4), C10–Co1 2.174(3), C11–C12 1.507(4), C21–C22 1.325(4), C21–S2 1.734(3), C22–C23 1.455(4), Co1–S1 2.308(1), C3–B3–C1 108.7(2), C3–B3–C2 119.1(2), S2–C2–C1 117.5(2), C9–C8–Co1 66.4(2), C10–C9–C8 118.8(3), C9–C10–C11 122.7(3), C18–C10–C11 113.7(3), C12–C11–C10 110.3(2), C22–C21–S2 118.3(2), C21–C22–C23 119.4(3), C9–Co1–S1 112.9(1).

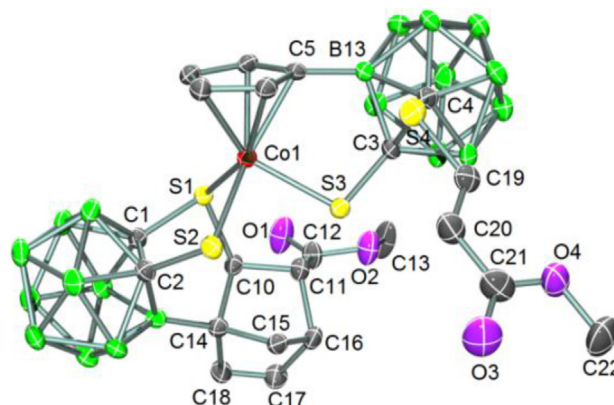


Fig. 6. Molecular structure of **6a**; ellipsoids show 30% probability levels, and the hydrogen atoms have been omitted for clarity. Selected bond lengths (Å) and angles (°): Co1–ring centroid 1.705(1), C5–B13 1.576(5), B3–C14 1.559(5), S1–C1 1.814(3), S1–C10 1.858(3), S1–Co1 2.284(1), S2–C2 1.782(3), S2–Co1 2.261(1), S3–C3 1.771(3), S3–Co1 2.275(1), S4–C19 1.752(4), S4–C4 1.766(4), C1–C2 1.665(4), C3–C4 1.806(5), C10–C11 1.542(4), C10–C14 1.576(4), C11–C12 1.497(5), C11–C16 1.567(4), C14–C15 1.527(4), C14–C18 1.541(4), C15–C16 1.532(4), C16–C17 1.515(4), C17–C18 1.316(5), C19–C20 1.288(5), C20–C21 1.460(6), C14–B3–C1 109.6(3), C14–B3–C2 122.6(3), C5–B13–C3 111.9(3), C5–B13–C4 123.6(3), C1–S1–C10 92.0(1), C1–S1–Co1 103.9(1), C10–S1–Co1 120.3(1), C2–S2–Co1 104.2(1), C3–S3–Co1 104.7(1), C19–S4–C4 103.6(2), S2–Co1–S3 85.4(4), S2–Co1–S1 89.7(3), S3–Co1–S1 103.5(4).

The hydrogens generated from [4 + 2] cycloaddition of the new *o*-carboranedithio moiety show corresponding resonance peaks, as shown in SI-Figure 3. The two new B–C bonds appear at 127.0 ppm for B(13)–C(5) and 52.3 ppm for B(3)–C(14) as characteristic broad signals in ^{13}C NMR. The B(3) and B(13) atoms show low-field shift around 0.8 ppm in the ^{11}B NMR, indicating the formation of these B–C bonds. The substituent at C(11) is not big enough to freeze configuration of the bicyclo-[2,2,1] unit. As the result, the solution of **6a** contains both *endo* and *exo* isomers, but *exo* species is the preferential configuration. The isolated *exo*-**6a** shows *exo*:*endo* = 3:1 in solution, whereas 1:1 ratio for the isolated *endo*-**6a** in solution. Each signal was identified by 2D COSY and HMQC. Compound **6b** was confirmed by spectral data (see Supporting information) which is similar to **6a** in structure.

2.1.5. Ligand exchange reactions

The chelating ability of in situ generated bulky dimercapto ligand in **6a/6b** is much weaker because of the electron deficiency of the adjacent carborane cage, allowing to be quickly and quantitatively replaced by the stronger chelating ligands **L1–L3** to yield **3a(L1–L3)** and **3b(L1–L3)** (Scheme 2 and Supporting information).

2.2. Proposed mechanisms

Both B–H and C–H activation as well as hydrogen transfer play key roles in the information of B–C coupled products. Therefore, a series of deuterium-labeling experiments and MS, NMR, GC monitoring reactions were performed to confirm the origin and destination of hydrogen transfer. Based on the series reactions of **1a**, the possible formation mechanisms of all the four types B–C coupled complexes were proposed.

2.2.1. Formation of 3a(L1)

2.2.1.1. Deuterium-labeled reaction. The reaction of **1a**, **2** and **L1** gave rise to product **3a(L1)**. From the X-ray structure of **3a(L1)** (Fig. 1) we can see that both B–H bond of carborane and C–H bond of Cp unit in **1a** have been activated to lose one hydrogen atom for each. Bronsted acid (**L1**) also loses one hydrogen atom as a

hydrogen source. The alkyne **2** is reduced by receiving one hydrogen atom as a hydrogen acceptor. Two hydrogen atoms might combine and become H₂ molecule. Therefore, a series of reactions were designed to prove possible pathways.

Firstly, we used the deuterated **d₁-L1** [(CH₂)₄NCS₂D] to react with **1a** and **2**. As a result, no proton was deuterated in the isolated product **3a(L1)**, indicating that **d₁-L1** is not the hydrogen source to reduce alkyne. We then used fully deuterated 16e starting compound **d₅-1a** [(d₅-Cp)CoS₂B₁₀H₁₀, D ≥ 75%] to react with **2** and **L1**. The product **d₄-3a(L1)** was isolated where no proton of the olefinic unit has been deuterated (see Fig. 7). This demonstrates that the Cp ring of **1a** is not the hydrogen source to reduce the alkyne either even although the Cp has lost one hydrogen atom in the reaction. If all the three reagents were deuterated, that is, **d₅-1a** (D ≥ 75%), **d₁-2** [DC≡CCO₂Me] and **d₁-L1** were used **d₅-3a(L1)** was isolated as determined by ¹H NMR (Fig. 8). This reveals that the normal proton at C(9) which has reduced the terminal alkyne come from the activated B(3)–H bond of the carborane cage.

2.2.1.2. Monitoring by EI-MS and GC. EI-MS and GC methods were used to monitor the reaction process of **1a**, **2** and **L1**. Initially a strong peak containing carborane and alkyne at 232.1 (*m/z*) was observed which corresponds to a stable organic fragment from intermediates **I** or/and **II** or/and **III** (Scheme 3). Later, the molecular ion peak at 559.1 (*m/z*) of **3a(L1)** and its fragments appeared. Note that the product **3a(L1)** started to form around 45 min and the reaction almost completed in 3 h by TLC test. By GC detection H₂ was unambiguously observed, as shown in SI-Chart 1 if the reaction was done in an autoclave.

2.2.1.3. Monitoring by ¹H NMR. The reaction of **1a**, **2** and **L1** in a J. Young valve NMR tube was detected by ¹H NMR at ambient temperature. The assignments for the characteristic protons of the intermediates **I**, **II** and **III** (Scheme 3) were shown in SI-Figure 2. The intermediate **I** from the alkyne addition was detected in the very earlier stage by its characteristic ¹H resonance at 6.65 ppm assigned to the HC=CCO₂Me unit as compared to a Me₅CpCo analog [44]. Later, broad hydride signals appeared in the region from –4 to –8 ppm, may be better expressed as Co–H–B. Very shortly (around 20 min) these hydride signals completely disappeared. At the same time **III** was observed owing to its characteristic doublets at 5.93 and 3.94 ppm with *J* = 10 Hz, parallel to those of a Me₅CpIr

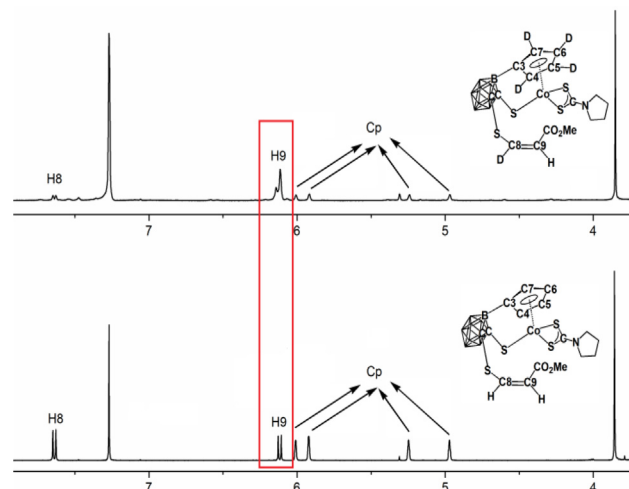


Fig. 8. ¹H NMR spectra (3.8–7.8 ppm) of compounds **3a(L1)** (bottom) and **d₅-3a(L1)** (top) in CDCl₃ at 20 °C.

analog [29]. However, shimming problems, due to the generation of paramagnetic Co²⁺ species in the by-reactions, led to a gradual worsening of the NMR spectrum. Thus we could not identify more additional intermediates by NMR. This effect was found to be reproducible.

On the basis of above experimental results, a plausible mechanism for the generation of **3a(L1)** is summarized in Scheme 3. The B–H activation at B(3) of the carborane and hydrogen transfer to the alkyne should occur as the earlier steps (**I**–**III**) after alkyne insertion into one Co–S bond, as previously reported [26–37,41,42] and revealed by these capture experiments. It should be noted that the iridium analog of intermediate **III** is rather stable [26–32], suggesting that the proposed cobalt intermediate is reasonable. The chelating coordination of **L1** would induce a change in the binding mode of Cp from η⁵ to η¹ (**IV-A**) [45–50], followed by α–H elimination (**V-A**) [51–54], H₂ release, Co–B and Co–C cleavage, B–C formation, and Cp switching back to η⁵ coordination [45–50], finally leading to **3a(L1)**.

2.2.2. Formation of **4a**

In contrast to **3a(L1)**, **4a** contains no chelating ligand **L4**. However, in the absence of **L4**, **4a** can not be generated. Series of reactions by deuterium-labeling reagents were designed to demonstrate hydrogen transfer, as shown in Fig. 9. For example, the ¹H NMR spectrum of **d₅-4a** generated from **d₅-1a** (No. 2 in Fig. 9) shows that one deuterium of **d₅-Cp** unit has been transferred to C(4) atom (see Fig. 4). Reaction of **1a**, **2** and **d₁-L4** led to non-deuterated **4a** (No. 3 in Fig. 9), which supports that the other hydrogen atom at C(4) coming from carborane, the same as in **3a(L1)**, other than from **L4**. Reaction of **1a**, **d₁-2** and **L4** gave rise to **d₁-4a** containing the deuterium at C(3). Thus the formation of **4a** is proposed in Scheme 3. **L4** chelates to metal (**IV-B**), same as **L1** in the formation of **3a(L1)**, to induce Cp ring slippage. Then the reduced alkyne replaces the weakly coordinating ligand **L4**, followed by the activated C–H from Cp transferring to C(4) to generate **4a**.

2.2.3. Formation of **5a(L6)/5a(L7)**

The same early stage for B–H activation as in the formation of **3a(L1)**, addition of (**L6**)/(**L7**) as 4e donor led to (**IV-C**) (Scheme 3), then the activated C–H from Cp migrates to form an allyl ligand in **5a(L6)/5a(L7)**.

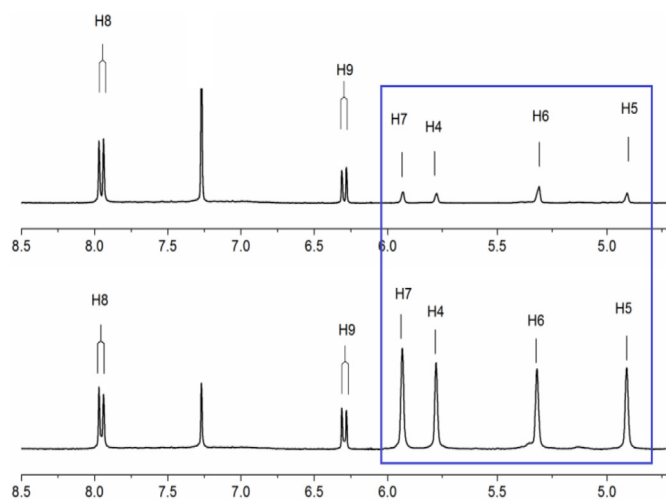
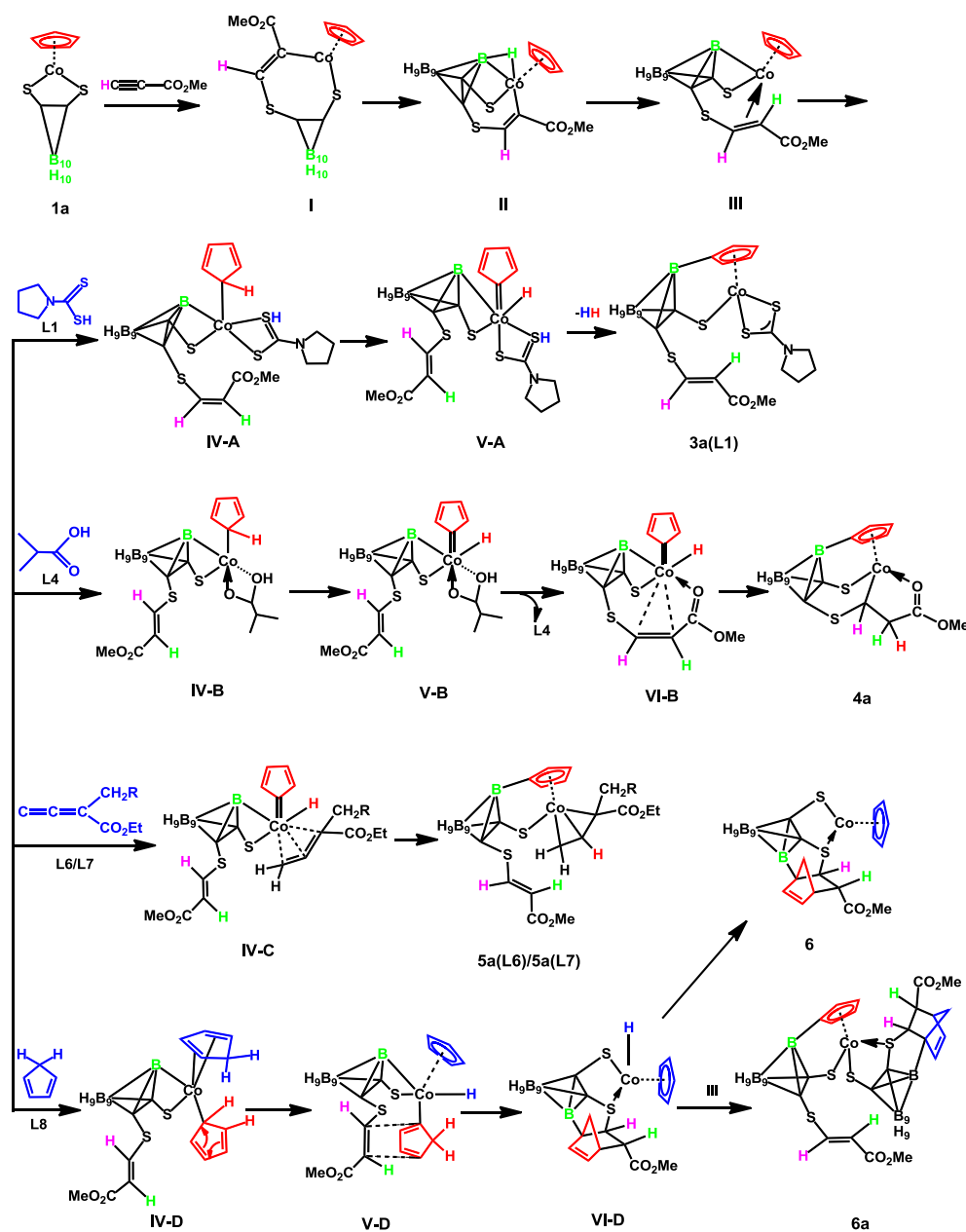


Fig. 7. ¹H NMR spectra (4.8–8.5 ppm) of compounds **3a(L1)** (bottom) and **d₄-3a(L1)** (top) in CDCl₃ at 20 °C.



Scheme 3. Proposed mechanisms for the formation of B–C containing carborane derivatives.

2.2.4. Formation of **6a**

2.2.4.1. Deuterium-labeled reaction. If **d₅-1a** (D-incorporation $\geq 95\%$) was used to react with **2** and **L8** product **d₉-6a** was isolated where the Cp ring and the Diels–Alder cycloaddition moiety were deuterated (see $^1\text{H NMR}$ in SI-Figure 3). This demonstrates that the existing $\text{d}_5\text{-Cp}$ ligand and the coordinating CpH (**L8**) are exchangeable. This experiment also supports oxidative addition of free CpH to metal to produce Cp as well as the exchange of η^5 - and η^1 -Cp binding modes and hydrogen 1,5-Sigmatropic shift over Cp ring driven by the further Diels–Alder cycloaddition. Using **d₁-2** led to **d₂-6a**. $^1\text{H NMR}$ (Fig. 10) shows that the hydrogen atoms at C(19) and C(10) are deuterated, reflecting that they originate from the terminal alkyne. But the hydrogen atoms at C(20) and C(11) are not deuterated.

2.2.4.2. Monitoring by EI-MS, GC and $^1\text{H NMR}$. In the earlier stage the peak at 232.1 (m/z) was observed which corresponds to a

fragment from **I** or **II** or **III** (2 h). But differently, in this reaction the molecular ion peak at 414.1 (m/z) for intermediate **III** could be observed for a long time (6 h) since this is a slow reaction in which **III** can survive longer. This is in a sharp contrast to the formation of **3a(L1)**, where the fast reaction makes observation of species **III** impossible. Compound **6** was observed from 2.5 h and **6a** was observed starting from 4.5 h, as confirmed by TLC. Note that only the fragment of **6a** can be observed by MS because of the weaker binding of the new-generated bulky dimercapped ligand. Production of H_2 as a by-product was confirmed by GC (see SI-Chart 2). Additionally, intermediate **I** was clearly observed by $^1\text{H NMR}$ in the earlier time, but the generated paramagnetic species badly disturbed shimming which prevented observation of more species.

Concerning the formation of **6a** (Scheme 3), the coordination of **L8** to Co induces the existing η^5 -Cp to change binding mode to η^1 to form **IV-D**. Subsequent oxidative addition of the bound CpH to the metal might occur [51–61], and the resulting η^1 -Cp might undergo

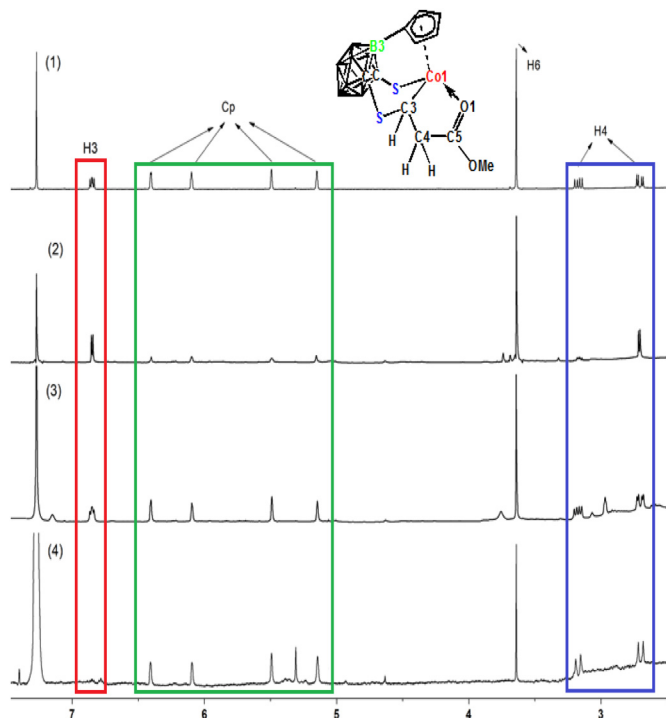


Fig. 9. ^1H NMR spectra (2.5–7.5 ppm) of the products from deuterium-labeling reactions in CDCl_3 at 20 °C. (1) **4a** (**1a** + **2** + **L4**); (2) **d₅-4a** (**d₅-1a** + **2** + **L4**); (3) **4a** (**1a** + **2** + **d₁** - **L4**); (4) **d₁-4a** (**1a** + **d₁** - **2** + **L4**).

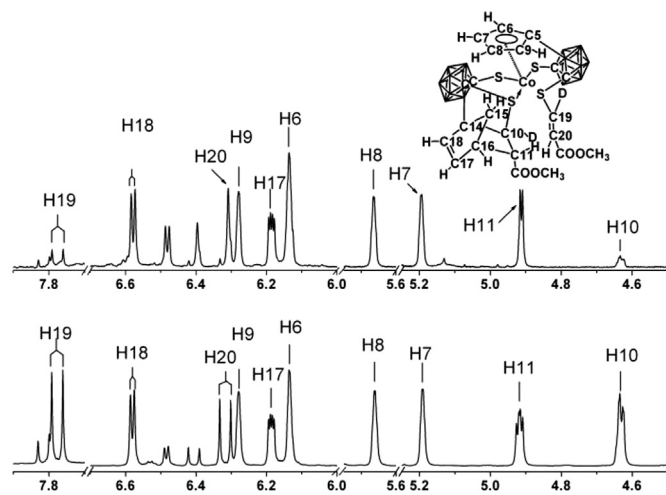


Fig. 10. ^1H NMR spectra (4.5–7.9 ppm) of **6a** (bottom) and **d₂-6a** (top) in CDCl_3 at 20 °C.

hydrogen 1,5-sigmatropic rearrangement [62,63] over the ring driven by the intramolecular [4 + 2] cycloaddition [64] with the olefinic unit (**V-D**). As a result, the hydride species (**VI-D**) is produced after cleavage of the Co–B and Co–C bonds. Its reductive elimination leads to paramagnetic species **6** and its further reaction with **III** gives rise to **6a**.

Using (MeCp)CoS₂C₂B₁₀H₁₀ (**1b**) instead of **1a** led to **6b**. This example exhibited an alternative pathway. MeCp remains intact and free CpH is oxidized to metal for further Diels–Alder addition because of forbidden methyl shift over the ring. Following the above procedure instead of **L8** by fresh MeCpH, no Diels–Alder reaction product could be isolated. This demonstrates that the

MeCp ring cannot undergo 1,5-Sigmatropic rearrangement over the ring, thus excluding the direct [4 + 2] addition of free MeCpH to the olefinic unit.

3. Conclusions

One-pot three-component reactions of 16-electron complex Cp[#]Co(S₂C₂B₁₀H₁₀) (Cp[#] = Cp, **1a**; MeCp, **1b**; Me₄Cp, **1c**; Me₅Cp, **1d**), methyl propiolate (HC≡CCO₂Me) and Bronsted acids (**L1–L8**) have been studied. A facile B–C bond formation between carboranedithiolate and Cp/MeCp has been observed through cobalt-induced and ligand-assisted both B–H and C–H activation at ambient temperature. This leads to selective B-functionalization of carborane by a metal-bound η⁵-Cp group in good yields. The methodology requires the suitable size of ancillary ligand, electron-deficient alkyne and 3e-donating Bronsted acid ligands, thus suitable for a broad range of substrates. Four types of products were obtained dependent on Bronsted acids. This work opens a way to development of new types of functional groups at a boron site of carborane.

4. General methods and synthesis

All manipulations were carried out under an argon atmosphere by using standard Schlenk techniques unless otherwise noted. Petroleum ether, diethyl ether, and tetrahydrofuran were dried over sodium and distilled under nitrogen. Hexanes and CH₂Cl₂ were dried over Na or CaH₂, respectively, and distilled under nitrogen. Methyl propiolate (Alfa Aesar) and n-BuLi (2.0 M in hexanes, Aldrich) were used as supplied. [CpCo(CO)I₂] and Cp[#]Co(S₂C₂B₁₀H₁₀) (**1a** – **1d**) were prepared by literature procedures [1]. The isotope-labeled analogs were prepared using the commercially available isotope-labeled starting materials.

All NMR spectra were obtained at ambient temperature on Bruker DRX-500 spectrometer. Chemical shifts are reported relative to CHCl₃/CDCl₃ (δ ¹H = 7.26 ppm, δ ¹³C = 77.0 ppm) and external Et₂O–BF₃ (δ ¹¹B = 0 ppm), respectively. The IR spectra were recorded on a Bruker Vector 22 spectrophotometer with KBr pellets in the 4000–400 cm⁻¹ region. The mass spectra were recorded on a Micromass GC-TOF for EI-MS (70 ev). Elemental analysis was performed in an elemental vario EL III elemental analyzer. X-ray crystallographic data were collected on a Bruker SMART Apex II CCD diffractometer using graphite-monochromated Mo-K α (λ = 0.71073 Å) radiation. The intensities were corrected for Lorentz-polarization effects and empirical absorption with the SADABS program [2]. The structures were solved by direct methods using the SHELXL-97 program [3]. Details regarding data collection of six complexes (**3a(L1)**, **3a(L2)**, **3b(L3)**, **4a**, **5a**, and **5a(L6)**) are provided in the CIF files (CCDC 809345, 774630, 828292, 812791, 774631, and 832876).

Preparation of **3a(L1-L3)** and **3b(L1-L3)**. To a mixture of **1a/1b** (0.4 mmol) and **2** (2 mmol) in CH₂Cl₂ (20 mL) **L1(L2,L3)** (0.6 mmol) was added under argon. The resulting solution was stirred at ambient temperature for 7 h. After removal of solvent, the residue was column chromatographed on silica and eluted with hexanes/CH₂Cl₂ (1: 2) to give **3a(L1-L3)** and **3b(L1-L3)**, respectively (54%–60%).

Preparation of **4a** and **4b**. To a mixture of **1a/1b** (0.4 mmol) and **L4/L5** (8 mmol) in CH₂Cl₂ (30 mL) **2** (0.8 mmol) was added under argon. The resulting solution was stirred at ambient temperature for 15 h. After removal of solvent, the residue was column chromatographed on silica and eluted with hexanes/CH₂Cl₂ (2: 1) to give **4a/4b** (45%–53%).

Preparation of **5a(L6)/5a(L7)**. To a mixture of **1a** (0.4 mmol) and **L6/L7** (8 mmol) in CH₂Cl₂ (20 mL) **2** (0.8 mmol) was added under

argon. The resulting solution was stirred at ambient temperature for 18 h. After removal of solvent, the residue was column chromatographed on silica and eluted with hexanes/CH₂Cl₂ (1: 1) to give 5a(L6)/5a(L7) (25%–51%).

Preparation of 6a/6b and 6. To a mixture of 1a/1b (0.4 mmol) and L8 (0.4 mmol) in CH₂Cl₂ (20 mL) 2 (0.8 mmol) was added under argon. The resulting solution was stirred at ambient temperature for 18 h. After removal of solvent, the residue was column chromatographed on silica and eluted with hexanes/CH₂Cl₂ (1: 1) to give 6a/6b (10%–23%) and 6 (10%–30%).

Additional details on the preparation and characterization of the complexes is available in the [Supporting Information](#).

Author information

The authors declare no competing financial interest.

Acknowledgment

This work was supported by the National Natural Science Foundation of China (21271102 and 21472086), the National Basic Research Program of China (2013CB922101), and the Natural Science Foundation of Jiangsu Province (BK20130054).

Appendix A. Supplementary data

Supplementary data related to this article can be found at <http://dx.doi.org/10.1016/j.jorgchem.2015.06.013>.

References

- [1] M.F. Hawthorne, *Angew. Chem. Int. Ed.* 32 (1993) 950–984.
- [2] M.F. Hawthorne, A. Maderna, *Chem. Rev.* 99 (1999) 3421–3434.
- [3] J. Plešek, *Chem. Rev.* 92 (1992) 269–278.
- [4] R.N. Grimes, *Coord. Chem. Rev.* 773 (2000) 200–202.
- [5] A.K. Saxena, J.A. Maguire, N.S. Hosmane, *Chem. Rev.* 97 (1997) 2421–2462.
- [6] V.I. Bregadze, I.B. Sivaev, S.A. Glazun, *Anti-Cancer Agents Med. Chem.* 6 (2006) 75–109.
- [7] J.F. Valliant, K.J. Guenther, A.S. King, P. Morel, P. Schaffer, O.O. Sogbein, K.N. Stephenson, *Coord. Chem. Rev.* 232 (2002) 173–230.
- [8] R.N. Grimes, *Carboranes*, Academic Press, New York, 2011.
- [9] K. Vyakaranam, J.B. Barbour, J. Michl, *J. Am. Chem. Soc.* 128 (2006) 5610–5611.
- [10] B. Grüner, Z. Janoušek, B.T. King, J.N. Woodford, C.H. Wang, V. Vsetečka, J. Michl, *J. Am. Chem. Soc.* 121 (1999) 3122–3126.
- [11] A.S. Larsen, J.D. Holbrey, F.S. Tham, C.A. Reed, *J. Am. Chem. Soc.* 122 (2000) 7264–7272.
- [12] Y.H. Zhu, C.B. Ching, K. Carpenter, R. Xu, S. Selvaratnam, N.S. Hosmane, J.A. Maguire, *Appl. Organomet. Chem.* 17 (2003) 346–350.
- [13] L.Y. Liang, A. Rapakousiou, L. Salmon, J. Ruiz, D. Astruc, B.P. Dash, R. Satapathy, J.W. Sawicki, N.S. Hosmane, *Eur. J. Inorg. Chem.* 20 (2011) 3043–3049.
- [14] C. Masalles, J. Llop, F. Teixidor, *Adv. Mater.* 14 (2002) 826–829.
- [15] J. Mola, E. Mas-Marza, X. Sala, I. Romero, M. Rodríguez, C. Viñas, T. Parella, A. Llobet, *Angew. Chem. Int. Ed.* 47 (2008) 5830–5832.
- [16] V.I. Bregadze, *Chem. Rev.* 92 (1992) 209–223.
- [17] A.V. Puga, F. Teixidor, R. Sillapää, R. Kivekäs, M. Arca, G. Barbera, C. Viñas, *Chem. Eur. J.* 15 (2009) 9755–9763.
- [18] J.D. Hewes, C.W. Kreimendahl, T.B. Marder, M.F. Hawthorne, *J. Am. Chem. Soc.* 106 (1984) 5757–5759.
- [19] S.W. Du, D.D. Ellis, P.A. Jelliss, J.A. Kautz, J.M. Malget, F.G.A. Stone, *Organometallics* 19 (2000) 1983–1992.
- [20] S.W. Du, J.A. Kautz, T.D. McGrath, F.G.A. Stone, *Chem. Commun.* 9 (2002) 1004–1005.
- [21] B.J. Meneghelli, R.W. Rudolph, *J. Am. Chem. Soc.* 100 (1978) 4626–4627.
- [22] M.G.L. Mirabelli, L.G. Sneddon, *J. Am. Chem. Soc.* 110 (1988) 449–453.
- [23] R. Wilczynski, L.Y. Sneddon, *Inorg. Chem.* 21 (1982) 506–514.
- [24] E.W. Corcoran Jr., L.G. Sneddon, in: J.F. Liebman, A. Greenberg, R.E. Williams (Eds.), *Advances in Boron and the Boranes*, VCR, New York, 1988, p. 71.
- [25] S. Chatterjee, P.J. Carroll, L.G. Sneddon, *Inorg. Chem.* 49 (2010) 3095–3097.
- [26] M. Herberhold, H. Yan, W. Milius, B. Wrackmeyer, *Angew. Chem.* Ed 38 (1999) 3689–3691.
- [27] M. Herberhold, H. Yan, W. Milius, B.Z. Wrackmeyer, *Anorg. Allg. Chem.* 626 (2000) 1627.
- [28] M. Herberhold, H. Yan, W. Milius, B. Wrackmeyer, *J. Organomet. Chem.* 604 (2000) 170–177.
- [29] M. Herberhold, H. Yan, W. Milius, B. Wrackmeyer, *Chem. Eur. J.* 6 (2000) 3026–3032.
- [30] M. Herberhold, H. Yan, W. Milius, B. Wrackmeyer, *J. Organomet. Chem.* 623 (2001) 149–152.
- [31] M. Herberhold, H. Yan, W. Milius, B. Wrackmeyer, *Chem. Eur. J.* 8 (2002) 388–395.
- [32] M. Herberhold, H. Yan, W. Milius, B. Wrackmeyer, *Dalton Trans.* 11 (2001) 1782–1789.
- [33] B.-H. Xu, D.-H. Wu, Y.-Z. Li, H. Yan, *Organometallics* 26 (2007) 4344–4349.
- [34] B.-H. Xu, X.-Q. Peng, Y.-Z. Li, H. Yan, *Chem. Eur. J.* 14 (2008) 9347–9356.
- [35] Y.-G. Li, Q.-B. Jiang, Y.-Z. Li, H. Yan, V.I. Bregadze, *Inorg. Chem.* 49 (2010) 4–6.
- [36] Y.-G. Li, Q.-B. Jiang, X.-L. Zhang, Y.-Z. Li, V.I. Bregadze, H. Yan, *Inorg. Chem.* 49 (2010) 3911–3917.
- [37] (a) G.-F. Liu, J.-R. Hu, J.-L. Wen, H.-M. Dai, Y.-Z. Li, H. Yan, *Inorg. Chem.* 50 (2011) 4187–4194; (b) Y.-J. Quan, Z.-W. Xie, *J. Am. Chem. Soc.* 136 (2014) 15513–15516.
- [38] D.-H. Wu, C.-H. Wu, Y.-Z. Li, D.-D. Guo, X.-M. Wang, H. Yan, *Dalton Trans.* (2009) 285–290.
- [39] D.-H. Wu, B.-H. Xu, Y.-Z. Li, H. Yan, *Organometallics* 26 (2007) 6300–6306.
- [40] D.-H. Wu, Y.-G. Li, Y.-Z. Li, H. Yan, *Inorg. Chem.* 47 (2008) 6524–6531.
- [41] R. Zhang, L. Zhu, Z.-Z. Lu, H. Yan, V.I. Bregadze, *Dalton Trans.* 41 (2012) 12054–12063.
- [42] R. Zhang, L. Zhu, G.-F. Liu, H.-M. Dai, Z.-Z. Lu, J.-B. Zhao, H. Yan, *J. Am. Chem. Soc.* 134 (2012) 10341–10344.
- [43] D.-H. Kim, J. Ko, K. Park, S. Cho, S.O. Kang, *Organometallics* 18 (1999) 2738–2740.
- [44] H.-D. Ye, G.-Y. Ding, M.-S. Xie, Y.-Z. Li, H. Yan, *Dalton Trans.* 40 (2011) 2306–2313.
- [45] J.M. O'Connor, C.P. Casey, *Chem. Rev.* 87 (1987) 307–318.
- [46] D.E. Herbert, M. Tanabe, S.C. Bourke, A.J. Lough, I. Manners, *J. Am. Chem. Soc.* 130 (2008) 4166–4176.
- [47] L.F. Veiros, *Organometallics* 19 (2000) 5549–5558.
- [48] W. Simanko, V.N. Sapunov, R. Schmid, K. Kirchner, *Organometallics* 17 (1998) 2391–2393.
- [49] G.K. Anderson, R.J. Cross, S. Fallis, M. Rocamora, *Organometallics* 6 (1987) 1440–1466.
- [50] T. Mizuta, Y. Imamura, K. Miyoshi, *J. Am. Chem. Soc.* 125 (2003) 2068–2069.
- [51] W. Simanko, W. Tesch, V.N. Sapunov, K. Mereiter, R. Schmid, K. Kirchner, *Organometallics* 17 (1998) 5674–5688.
- [52] M. Brookhart, B.E. Grant, C.P. Lenges, M.H. Prosenc, P.S. White, *Angew. Chem. Int. Ed.* 39 (2000) 1676–1679.
- [53] E.K. Byrne, K.H. Theopold, *J. Am. Chem. Soc.* 109 (1987) 1282–1283.
- [54] E.K. Byrne, K.H. Theopold, *J. Am. Chem. Soc.* 111 (1989) 3887–3896.
- [55] H. Werner, *Organometallics* 24 (2005) 1036–1049.
- [56] M.A. Esteruelas, A.M. López, *Organometallics* 24 (2005) 3584–3613.
- [57] Y. Sun, H.-S. Chan, H. Zhao, Z. Lin, Z. Xie, *Angew. Chem. Int. Ed.* 45 (2006) 5533–5536.
- [58] J.S. Merola, R.T. Kacmarcik, *Organometallics* 8 (1989) 778–784.
- [59] J.W. Ho, Z.M. Hou, R.J. Drake, D.W. Stephan, *Organometallics* 12 (1993) 3145–3157.
- [60] C.Y. Tang, W. Smith, A.L. Thompson, D. Vidovic, S. Aldridge, *Angew. Chem. Int. Ed.* 50 (2011) 1359–1362.
- [61] S. Aldridge, D.L. Kays, A. Al-Fawaz, L.M. Jones, P.N. Horton, M.B. Hursthouse, R.W. Harrington, W. Clegg, *Chem. Commun.* 24 (2006) 2578–2580.
- [62] I.D. Gridnev, *Coord. Chem. Rev.* 252 (2008) 1798–1818.
- [63] H. Shen, H.-S. Chan, Z. Xie, *J. Am. Chem. Soc.* 129 (2007) 12934–12935.
- [64] N.M. Boag, K.M. Rao, *Chem. Commun.* 12 (2009) 1499–1501.